

Maximum and Geometric-Mean Spectral Demands in the Near-Fault Region

Yin-Nan Huang¹⁾, Andrew Whittaker¹⁾ and Nicolas Luco²⁾

1) Dept. of Civil, Structural, Environmental Engineering, University at Buffalo, State University of New York, Buffalo, NY

2) United States Geological Survey, Denver, CO

ABSTRACT

The Next Generation Attenuation (NGA) models for shallow crustal earthquakes in the Western United States, like most other ground motion attenuation relationships, predict the *geometric mean* of horizontal spectral demand. In the near-fault region, the geometric mean spectral demand can be much smaller than the *maximum* spectral demand for a pair of ground motions. One hundred and forty seven pairs of ground motion records for earthquakes with moment magnitude greater than 6.5 and site-to-source distance smaller than 15 km were selected from the NGA strong motion dataset to study the relationship between maximum and geometric mean demands. The ratio of maximum to geometric mean spectral demand for each pair of ground motions was calculated. The ratio showed clear dependency on period and the Somerville directivity parameters. In a median sense, the geometric mean from the NGA models conservatively predicts the maximum spectral demand at 0.1 and 0.2 seconds and underestimates the maximum demand for periods of 0.5 and greater.

INTRODUCTION

The U.S. Nuclear Regulatory Guide 1.165 [1] includes procedures for determining a design spectrum for the Safe Shutdown Earthquake (SSE) based on the spectral demand for a median return period of 100,000 years. Attention is focused on the short period range of 0.1 to 1 second because this range includes the first mode period of most nuclear structures.

Next Generation Attenuation (NGA) models have been proposed for shallow crustal earthquakes in the Western United States. The spectral demand predicted by the NGA models is termed *GMRotI50*, which is similar to the *geometric mean* (or *geomean*) of the spectral ordinates for a pair of ground motions. The 2007 United States Geological Survey (USGS) seismic hazard maps will utilize the NGA models for characterizing seismic hazard in the Western US. However, in the near-fault region, the geomean spectral demand can be much smaller than the *maximum* spectral demand for a pair of motions.

This study seeks to identify a) the ratio of the maximum spectral demand to GMRotI50 with emphasis on the short period range, which is of importance for safety-related nuclear structures, and b) the impact on SSE shaking demands if maximum demand is used instead of geometric mean demand. A large number of pairs of near-fault ground motion records were selected and the ratio of the maximum spectral demand to GMRotI50 for each pair of motions was calculated. The study is reported in more detail in Huang et al. [2, 3].

NEXT GENERATION ATTENUATION RELATIONSHIPS AND GMRotI50

The three NGA relationships that the USGS has adopted to generate the 2007 seismic hazard maps for the Western US were developed by Boore and Atkinson [4], Campbell and Bozorgnia [5], and Chiou and Youngs [6]. Information on the relationships is available at http://peer.berkeley.edu/products/rep_nga_models.html. The ground motions used to develop these relationships were extracted from the PEER NGA database (<http://peer.berkeley.edu/nga/>), which includes more than 3500 sets of recordings from 173 earthquakes. Importantly, the database includes a significant number of near-fault recordings.

The geomean (square root of the product) of the spectral demands of two orthogonal horizontal components of ground motions is generally used as the response variable in attenuation relationships. It produces smaller aleatory uncertainty in the attenuation relationship compared to almost all other measures, such as 1) the maximum spectral demand across the two horizontal components, 2) the random horizontal demand, 3) strike-normal demand and 4) strike-parallel demand [7]. However, the value of the geomean demand will depend on the orientation of the sensors recording the earthquake shaking, especially for recordings with two strongly polarized components. In such cases, the spectral demand along one axis of the sensor might be much larger than that on the orthogonal axis, resulting in a geometric mean demand that is much smaller than the maximum demand and the arithmetic mean demand.

To address this potential drawback in the use of the geomean, Boore et al. [8] defined a rotated geomean that was independent of the sensor orientation. The rotated geomean is denoted as *GMRotI50*, where *GM* denotes Geometric Mean, *Rot* denotes that rotations over all non-redundant angles (0° through 90°) are considered, *I* identifies that period-independent rotations are used, and 50 identifies the median across all rotations. Boore et al. showed that the average effect of rotating the geomean on spectral demand was less than 3%.

The Fortran codes for the three NGA relationships provided by Stephen Harmsen of the USGS were modified for this study. Both the USGS codes and our Fortran codes predict median and logarithmic standard deviation for GMRotI50 for a combination of variables (e.g., moment magnitudes (M_w), closest site-to-fault-rupture distance (r), the average shear-wave velocity in the upper 30 meters of the soil column (V_{s30}), period and fault type).

MAXIMUM SPECTRAL DEMAND

Maximum shaking was defined in a spectral sense for this study. The procedure used to compute maximum and minimum spectral demands for a given period and pair of earthquake records is illustrated in part in Fig. 1. A 5%-damped 2-degree-of-freedom linear oscillator with a period of 1-second in both horizontal directions was subjected to the X and Y components of a sample ground motion. Fig. 1 presents the acceleration orbit of the oscillator with respect to the X and Y directions. The maximum acceleration (solid circle in the upper-left quadrant in this figure) and its orientation (α) with respect to the Y direction is identified by the point on the orbit farthest from the origin). The minimum spectral demand was taken as the peak spectral demand on the orthogonal component. In this study, the process was repeated at all periods considered in the analysis, from 0 to 1 second, to construct the *maximum* spectrum for the ground-motion pair. (The calculations were performed for periods ranging from 0 to 4 seconds; see Huang et al. [2, 3] for results for periods greater than 1 second.) For a given ground-motion pair, α varies as a function of period¹.

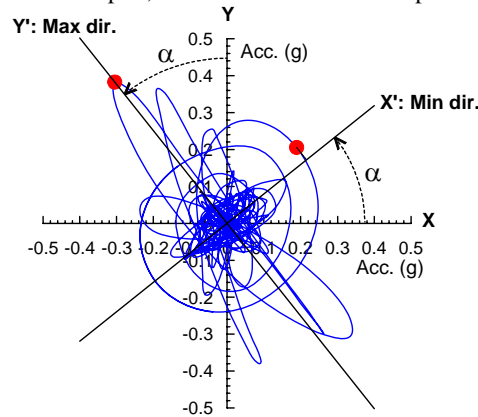


Fig. 1. Acceleration orbit of a 2-degree-of-freedom oscillator to compute maximum spectral demand

STRONG MOTION DATASET

The dataset used in this study is based on the PEER NGA ground motion database. Since the focus of our work was near-fault shaking, all pairs of ground motions from earthquakes with M_w of 6.5 and greater, and r of 15 km and less, were extracted for inclusion in our dataset. The list for the 147 ground-motion pairs in the dataset can be found in Huang et al. [2]. Each pair of time series was rotated to be strike-normal and strike-parallel to the causative fault by the PEER researchers. Of the 147 pairs of motions, 46 are associated with strike-slip faulting and 101 with dip-slip faulting; 56 pairs of motions are from the 1999 Chi-Chi earthquake in Taiwan.

¹ An alternate approach to compute maximum spectral demand is to rotate the two horizontal components of the earthquake record in small increments from 0° through 90°, 2) compute the spectral demand for each component and each angle of rotation, and 3) extract the maximum spectral demand from the data as a function of period. The two procedures will produce identical maximum demands but the algorithm used by the authors is computationally more efficient.

THE RATIO OF MAXIMUM SPECTRAL DEMAND TO MAXIMUM-MINIMUM GEOMEAN DEMAND

Fig. 2 presents the distribution of the ratio of maximum spectral demand to the geometric mean of the maximum and minimum demands for all 147 pairs of records in the dataset. The statistical interpretation of the ratios of spectral demands presented in this paper assumed that the ratios are lognormally distributed, and therefore median, β , 84th and 16th percentile results were computed using equations (1) through (4). Counted percentiles, which do not significantly change the conclusions drawn here based on the lognormal assumption, are presented in [3].

$$\theta_m = \exp\left(\frac{1}{n} \sum_{i=1}^n \ln y_i\right) \quad (1)$$

$$\beta = \sqrt{\frac{1}{n-1} \sum_{i=1}^n (\ln y_i - \ln \theta_m)^2} \quad (2)$$

$$y_{84th} = \theta_m \cdot e^{\beta} \quad (3)$$

$$y_{16th} = \theta_m \cdot e^{-\beta} \quad (4)$$

where n is the total number of pairs of ground motions; y_i is the ratio of spectral demands for the i th ground-motion pair; and θ_m , β , y_{16th} and y_{84th} are the median, logarithmic standard deviation, 16th percentile and 84th percentile of the ratio, respectively. In Fig. 2, the median values of the ratio for periods smaller than 0.2 second are about 1.2 and increase to 1.3 for periods greater than 0.4 second. These results show that, in the near-fault region, maximum spectral demand is 20% to 30% greater than the geomean demand in the period range of interest for most nuclear structures.

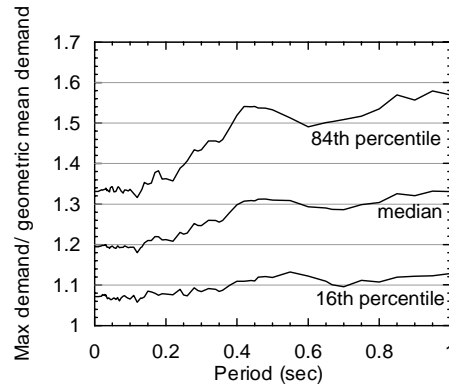


Fig. 2. Median, 84th and 16th percentiles of the ratio of maximum to geomean spectral demands for all the records in the dataset

THE RATIO OF MAXIMUM SPECTRAL DEMAND TO GMRotI50_ave

Results for all records in the dataset

For each pair of ground motions in the dataset, the parameters, such as M_w , r , V_{s30} and fault type, were extracted from the NGA Flatfile (http://peer.berkeley.edu/products/rep_nga_models.html) and used as input to the Fortran codes for the NGA relationships to generate GMRotI50 at periods of 0, 0.05, 0.1, 0.2, 0.3, 0.5 and 1 second. Values of GMRotI50 from each of the three NGA relationships were equally weighted; the resulting geomean was termed GMRotI50_ave. The ratio of maximum spectral demand to GMRotI50_ave for each pair of ground motions and each period was computed and the distribution of the ratio was calculated per (1) through (4). The solid lines in Fig. 3 show the median and 84th percentile of the ratio as a function of period. In a median sense, GMRotI50_ave overestimates the maximum demand by 10% at a period

of 0.2 second and underestimates the maximum demand by 30% at a period of 1 second. Columns 2 and 3 in Table 1 list the median and 84th percentile of the ratio of maximum spectral demand to GMRotI50_ave at 0.1, 0.2, 0.5 and 1.0 seconds for all ground-motion pairs in the dataset.

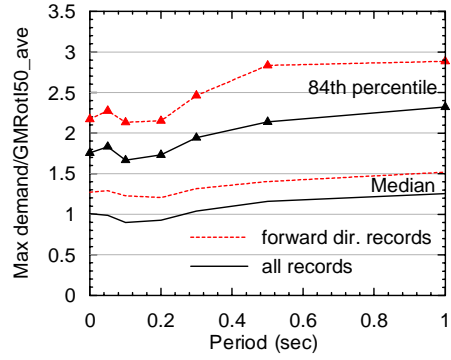


Fig. 3. Median and 84th percentile of the ratio of maximum spectral demand to GMRotI50_ave for all of the records and for the forward directivity records in the dataset

Table 1. Median and 84th percentile of the ratio of maximum spectral demand to GMRotI50_ave demand

Period (second)	Maximum demand/GMRotI50_ave			
	All records		Forward directivity records	
	Median	84th percentile	Median	84th percentile
0.1	0.9	1.7	1.2	2.1
0.2	0.9	1.7	1.2	2.2
0.5	1.2	2.1	1.4	2.8
1	1.3	2.3	1.5	2.9

Fault rupture directivity

Somerville et al. [9] developed a rupture directivity model that utilized a length ratio for strike slip faults, X ; a width ratio for dip-slip faults, Y ; an azimuth angle between the fault plane and ray path to site for strike-slip faults, θ ; and a zenith angle between the fault plane and ray path to the site for dip-slip faults, ϕ . Fig. 4 identifies these variables. Two parameters were used to characterize directivity effects: $X \cos \theta$ for strike-slip faults and $Y \cos \phi$ for dip-slip faults. Somerville observed that 1) for moment magnitude greater than 6.5, periods greater than 0.6 second and $X \cos \theta$ or $Y \cos \phi$ greater than about 0.5, the geomean horizontal spectral demand was on average greater than that predicted by the widely used attenuation relationship of Abrahamson and Silva [10], and 2) for moment magnitude greater than 6, periods greater than 0.5 second and θ or ϕ smaller than 45° , the strike-normal spectral demand was on average greater than the geomean horizontal spectral demand.

To consider the effect of the Somerville directivity parameters on the spectral demand, all records in the dataset with $X \cos \theta$ or $Y \cos \phi$ greater than or equal to 0.5 (forward directivity region) were selected for analysis. This bin of ground motions contains 50 pairs of records, all with θ or ϕ smaller than 45° .

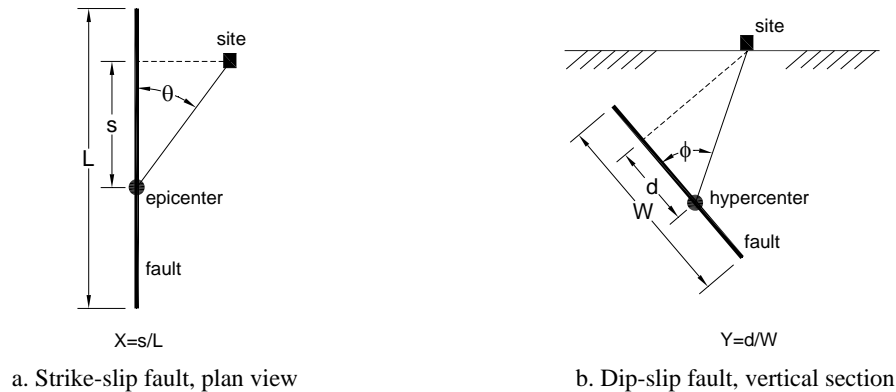


Fig. 4. Somerville directivity parameters (adapted from Somerville et al. [9])

Results for forward directivity records in the dataset

The analysis of Fig. 3 for all 147 pairs of ground motions was repeated for the 50 pairs of ground motions in the forward directivity region and the results are shown by the dashed lines in Fig. 3. The median and 84th percentile values of the ratio are 1.2 and 2.2, respectively, at a period of 0.2 second and 1.5 and 2.9, respectively, at a period of 1 second. Columns 4 and 5 in Table 1 list the median and 84th percentile of the ratio at 0.1, 0.2, 0.5 and 1.0 seconds. The results in Fig. 3 clearly show that maximum demand is a function of period and the Somerville directivity parameters in the near-fault region.

To further study the relationship between spectral demand in the near-fault region and the Somerville directivity parameters, the residual defined as the natural logarithm of the ratio of maximum spectral demand to $GMRotI50_{ave}$, that is, $LN(\text{maximum demand}/GMRotI50_{ave})$, was plotted as a function of $X \cos \theta$ and $Y \cos \phi$ and/or period in Figs. 5 and 6. The solid black dots in panels a and b of Fig. 5 show the 147 realizations for the residuals at periods of 0.2 and 1 seconds, respectively, and a linear least squares (LLS) fit to the data at each period. Fig. 5c shows the LLS fits at periods of 0.1, 0.2, 0.5 and 1 seconds to identify the effect of period on the residuals. Fig. 5d is the exponential of the values shown in Fig. 5c (which is equivalent to the ratio of maximum demand to $GMRotI50_{ave}$) and presents results in a linear scale. The surface shown in Fig. 6 is constructed using the regressed lines at all periods considered in the study. The ratio of maximum spectral demand to $GMRotI50_{ave}$ demand increases as $X \cos \theta$ or $Y \cos \phi$ increases and, for periods greater than 0.2 second, the ratio increases as the period increases. On average, for periods of 0.1 and 0.2 seconds, $GMRotI50_{ave}$ overestimates maximum spectral demand for $X \cos \theta$ and $Y \cos \phi$ smaller than 0.7 and underestimates that for $X \cos \theta$ and $Y \cos \phi$ greater than 0.7; for periods of 0.5 and 1 seconds, $GMRotI50_{ave}$ underestimates maximum demand throughout most of the range of $X \cos \theta$ and $Y \cos \phi$.

CLOSING REMARKS

One hundred and forty seven pairs of ground motion records with M_w greater than 6.5 and r smaller than 15 km were selected from the NGA strong motion dataset. The ratio of maximum spectral demand to maximum-minimum geomean demand for each pair of ground motions was calculated. The results show that maximum spectral demand is systematically greater than the maximum-minimum geomean demand by 20% to 30%. This study also reported the ratio of maximum to $GMRotI50_{ave}$ demand for each of the 147 pairs of ground motions and showed that the ratio is dependent on period and the Somerville directivity parameters. In a median sense, the ratio of maximum to $GMRotI50_{ave}$ spectral demand increases as $X \cos \theta$ or $Y \cos \phi$ increases and, for periods greater than 0.2 second, the ratio increases as the period increases; $GMRotI50_{ave}$ conservatively predicts the maximum spectral demand at 0.1 and 0.2 seconds for values of $X \cos \theta$ and $Y \cos \phi$ smaller than 0.7 (but not greater than 0.7), and underestimates the maximum demand for periods of 0.5 and 1 second across most of the range of $X \cos \theta$ and $Y \cos \phi$.

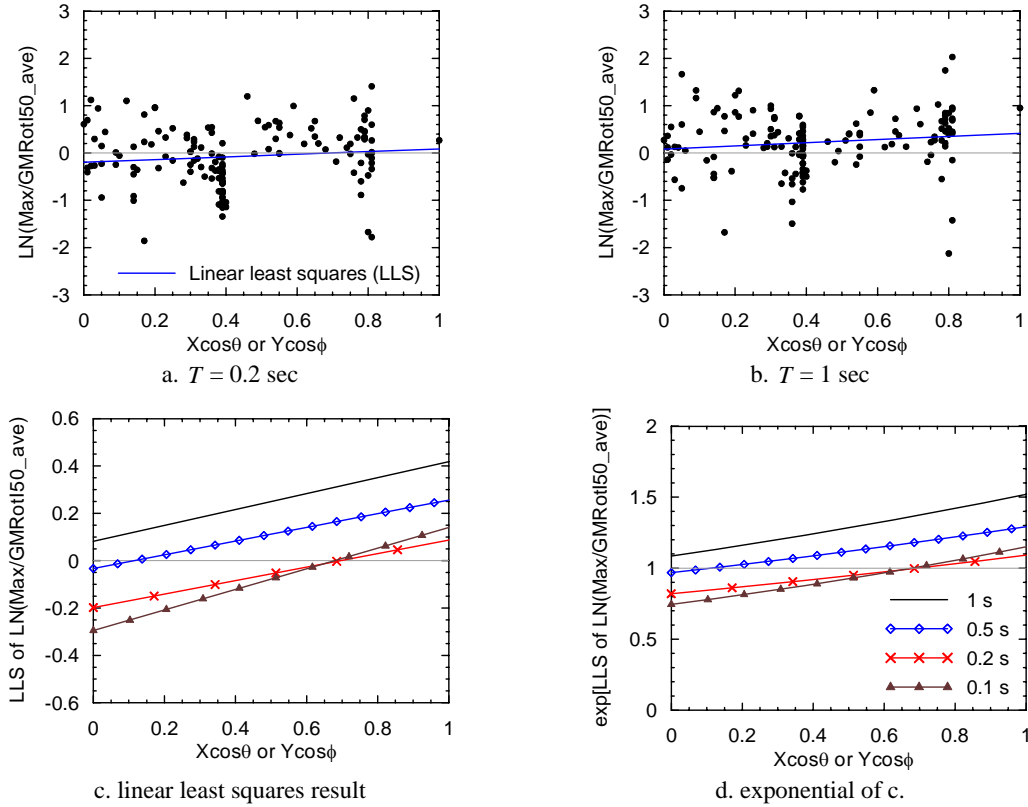


Fig. 5. Ratios of the maximum spectral demand to GMRotI50_ave at periods of 0.2 and 1 second and the linear least squares fits as a function of period and the Somerville directivity parameters

If maximum spectral demand and not geomean demand is to be considered for design of nuclear structures, attenuation relationships that predict maximum demand should be developed and then implemented in PSHA codes. Maximum spectral demand for a given median return period can be *estimated* by increasing the PSHA-based predictions for GMRotI50_ave by the factors presented in either column 2 of Table 1 for average directivity demand or column 4 of Table 1 for forward directivity demand. However, we note that the maximum demand *estimated* using this simple procedure will be different from that calculated by a PSHA using attenuation relationships that predict maximum spectral demand, unless the ratio of maximum spectral demand to GMRotI50_ave is independent of M_w and r (and any other variables used in the attenuation relationships) and the dispersion in the maximum spectral demand is equal to that in GMRotI50_ave.

ACKNOWLEDGEMENT

The original Fortran codes for the three NGA relationships were provided by Stephen Harmsen of the USGS. The authors acknowledge his important contribution to this study and appreciate his support and counsel over the duration of the study.

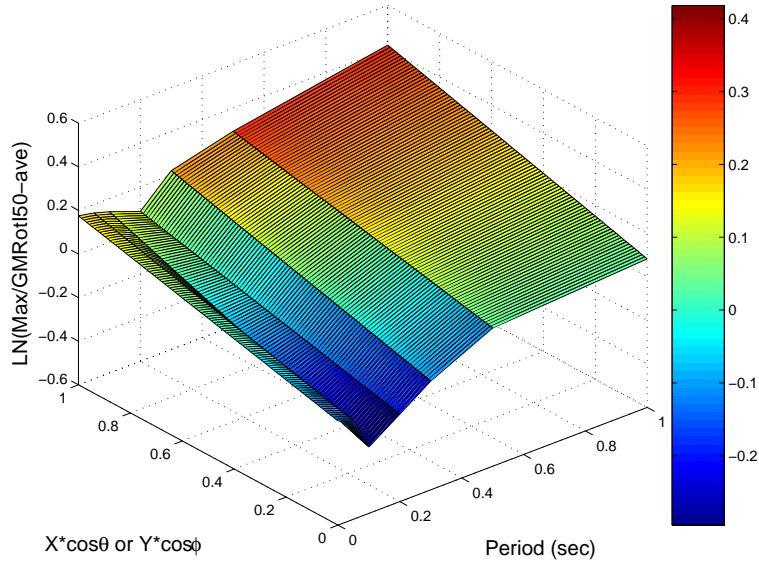


Fig. 6. Linear least squares fits of the ratios of the maximum spectral demand to GMRot150_ave as a function of period and the Somerville directivity parameters

NOMENCLATURE

d	Defined in Fig. 4b.
L	Defined in Fig. 4a.
M_w	Moment magnitude.
n	Total number of pairs of ground motions.
r	Closest site-to-source distance.
s	Defined in Fig. 4a.
W	Defined in Fig. 4b.
X	Length ratio for strike-slip faults, see Fig. 4a.
Y	Width ratio for dip-slip faults, see Fig. 4b.
V_{S30}	Average shear-wave velocity in the upper 30 meter of the soil column.
y_i	Ratio of the spectral demands for the i th ground-motion pairs.
y_{16th}	16th percentile of the ratio of the spectral demands.
y_{84th}	84th percentile of the ratio of the spectral demands.
α	Rotation angle to the maximum-demand direction for a pair of ground motions; see Fig. 1.
β	Logarithmic standard deviation of the ratio of the spectral demands.
ϕ	Zenith angle between fault plane and ray path to site for dip-slip faults; see Fig. 4b.
θ	Azimuth angle between fault plane and ray path to site for strike-slip faults; see Fig. 4a.
θ_m	The median of the ratio of the spectral demands of interest.

REFERENCES

1. Nuclear Regulatory Commission (USNRC). (1997). "Identification and characterization of seismic sources and determination of safe shutdown earthquake ground motion." *Regulatory Guide 1.165*, Washington, D.C.
2. Huang, Y.-N., Whittaker, A. S., and Luco, N. (2007). "NGA relationships, USGS seismic hazard maps, near-fault ground motions and site effects." Draft report under review for possible publication as a United States Geological Survey Open File Report.
3. Huang, Y.-N., Whittaker, A. S., and Luco, N. (2008). "Maximum spectral demands in the near-fault region." Paper in preparation, *Earthquake Spectra*.
4. Boore, D. M., and Atkinson, G. M. (2006). "Boore and Atkinson provisional NGA empirical ground-motion model for the average horizontal component of PGA, PGV and SA at spectral periods of 0.05, 0.1, 0.2, 0.3, 0.5, 1, 2, 3, 4 and 5 seconds." *NGA report*, Pacific Earthquake Engineering Research Center, Berkeley, California.
5. Campbell, K. W., and Bozorgnia, Y. (2006). "Campbell and Bozorgnia NGA empirical ground motion model for the average horizontal component of PGA, PGV, PGD and SA at selected spectral periods ranging from 0.01-10.0 seconds (version 1.0)." *NGA report*, Pacific Earthquake Engineering Research Center, Berkeley, California.
6. Chiou, B. S.-J., and Youngs, R. R. (2006). "Chiou and Youngs PEER-NGA empirical ground motion model for the average horizontal component of peak acceleration and pseudo-spectral acceleration for spectral periods of 0.01 to 10 seconds." *NGA report*, Pacific Earthquake Engineering Research Center, Berkeley, California.
7. Beyer, K., and Bommer, J. J. (2006). "Relationships between median values and between aleatory variabilities for different definitions of the horizontal component of motion." *Bulletin of the Seismological Society of America*, 96(4A), 1512-1522.
8. Boore, D. M., Watson-Lamprey, J., and Abrahamson, N. A. (2006). "Orientation-independent measures of ground motion." *Bulletin of the Seismological Society of America*, 96(4A), 1502-1511.
9. Somerville, P. G., Smith, N. F., and Graves, R. W. (1997). "Modification of empirical strong ground motion attenuation relations to include the amplitude and duration effects of rupture directivity." *Seismological Research Letters*, 68(1), 94-127.
10. Abrahamson, N., and Silva, W. J. (1997). "Empirical response spectral attenuation relations for shallow crustal earthquakes." *Seismological Research Letters*, 68(1), 94-127.